ENGINEERED, CAGE DESIGN IMPROVES EFFICIENCY FOR COMBATIVE ROD PUMP WELLS

Ramamurthy Narasimhan

Harbison-Fischer, a ChampionX business unit

ABSTRACT

Rod pumps often fail due to gas and solid interference. When the system's standing and traveling valves are unable to displace these solids or gas it can cause failure and severe damage to the overall rod pump system, such as intense ball rattling, plugged cages, inefficient pump fillage, and fluid pounding.

Historically, the industry has overcome these issues by utilizing stellite-lined and insert-guided cages with alterations for the ball's clearance. However, these offerings have only supplied a linear fluid path through the restricted valve areas. By changing the fluid flow path profile, cages can improve their flow coefficient and more efficiently contain gas and solids in the fluid flow path. Additionally, by optimizing the flow design and creating a shorter ball travel length, Harbison-Fischer's HFX cage reduces gas and solid interference by lowering the pressure drop during valve actuation, improving the overall run-time and pumping efficiency.

A rod pump's performance depends on its ability to open and close valves during production operations regardless of the well's conditions. The HFX cage delivers a higher lifting force maximizing pump fillage and overall performance.

This white paper aims to define the variables and understand the factors affecting the coefficient of volume (Cv) of a cage used in rod lift applications. This understanding will help predict the pressure losses in different pumping well conditions and help optimize the system's efficiencies. Four variables will be discussed in this paper to identify an improved rod pump cage design: 1) pressure drop in a ball type cage 2) net lifting force and coefficient of lift on the ball 3) fluid tracing and untracing on a ball surface 4) changes in ball resistance through the cross-sectional area. These four variables will be explained with a general engineering equation, a finite element analysis, or a laboratory model with defined test parameters. The finite element analysis is used when general engineering formulas cannot meet the fluid flow conditions. Similarly, the finite element analysis has few limitations to replicate actual well conditions for this study. Understanding these general engineering and test analyses is critical to understand a cage's efficiency and loss.

INTRODUCTION

Sucker rod pumps typically contain a reciprocating plunger inside a barrel, each connected to either a standing valve or traveling valve forming an internal compression chamber. Sucker rod pumps operate on the positive-displacement principle; inflow of well fluids from a low-pressure reservoir into an internal barrel compression chamber during the rod pump's upstroke, then, pumping the fluid into an outlet high-pressure fluid column during the rod pump’s downstroke. The reciprocating action of the plunger drives the expansion and the contraction of the internal compression chamber, while the synchronized action of the valves controls the intake of fluid from the low-pressure reservoir and the discharge of fluid to the high-pressure column. The ball type, one-way cages comprise of a ball and a seat and are the standard in sucker rod pumped wells.

The one-way cage influences the performances and run-times of a sucker rod pump cage. These cages are influenced by several factors, such as corrosion, erosion, abrasion, gas interference, and embedded solids. The ball’s restricted region is the fluid flow passage along the ball’s travel length in a completely assembled cage. This restricted region can be tested for its durability, speed of actuation, and reduced pressure drops or pressure gradients. The cage’s restricted region and the performance/challenges in various well conditions are described in the three subheadings below.

FINITE ELEMENT ANALYSIS METHOD

Finite element analysis on the fluid flow path boundary condition and on the ball restriction boundary condition will be explained in the respective analysis described in the subheading titled 2&3. The fluid media for all finite element analyses is water at room temperature with a specific gravity of 1.0. All analyses done with the standing valve (SV) and traveling valve (TV) are in vertical condition with the gravitation force assigned to the ball. Ansys and Solid Works flow simulation were used to develop this white paper.

LAB TEST METHOD

The lab test was done using a test setup as shown in **Figure 1.1**. The hydraulic fluid is pumped by (P1) through the manually operated flow control directional valve (V1) in series through a digital flow volume measuring sensor (FM1) and is connected to the inlet of the cage. The fluid pressure before and after the cage is measured by two pressure transducers (PT1 & PT2) that are parallelly connected to the fluid line 10-12” away from the cages (inlet & outlet) to read a stabilized inlet and outlet pressure (psi). The difference between the inlet pressure (psi) and outlet pressure (psi) is the pressure drop (psi) recorded for all cage configurations for the respective set flow rate. After completing the reading for one flow rate, the flow through the cage is increased by throttling the flow escaping the needle flow control valve (FC1). A 10-15 second delay is needed to stabilize the cage inlet flow and pressure before recording the next pressure drop. This pressure drop process and recording test was carried out from a flow rate of 15 GPM to 55 GPM in increments of 5 GPM. The test is repeated several times in the same process to record the average pressure

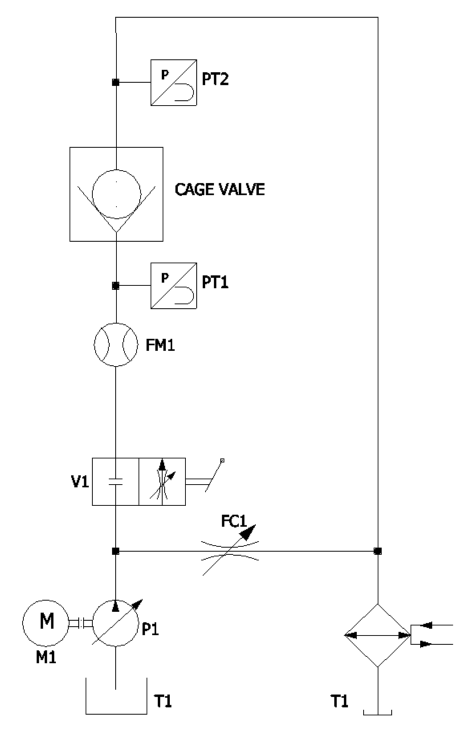

FIGURE 1.1

drop and minimize the test variance. During this testing, the fluid temperature is maintained at ±5°F from room temperature with a heat exchanger cooling the reservoir fluids that are returning to the tank.

All three methods (General engineering formula + FEA analysis + Lab Results) to be understood before making any judgements.

1. The work done by the fluid on the cage restriction (pressure drop)

1.1 API vs. alternate ball

The barrel's bottom is connected to the standing valve (SV). The closed state of the SV occurs when the ball seals to the seat's lapped surface due to the ball mass (m) and the fluid column above the ball (dead zone). To crack open the standing valve, the pump intake pressure (PIP) should be greater than, the sum of the ball mass and dead zone fluid force (sealing pressure). The pump intake pressure/reservoir pressure (PIP) will vary based on the well's fluid level and the dissolved and undissolved gas in the fluid. The higher the dissolved gas percentage, the lower the PIP. The standing valve ball mass must be selected for the dissolved gas percentage to open the standing valve with dynamic PIP well conditions (PIP > Ball mass+ (dead zone pressure X Ball Ø).

The traveling valve seat experiences sealing pressure due to the ball mass (m) and fluid head above the traveling valve. The pump's discharge pressure (Pd) should be greater than, the sum of the ball mass, and the fluid head pressure to open the traveling valve for fluid pumping. The type of ball in the traveling valve has a minimum contribution to increase the discharge pressure (Pd) when compared to the fluid head impact above the traveling valve. (Pd > Ball mass + (fluid head column pressure X ball Ø)).

The seat is dual lapped with an API &alternate pattern ball and seat. **Figure 1.2** shows the ball diameter as an Alt and API ball interfacing area. The mass of the 1.0" alternate ball is 65 grams (0.1433lb), and the mass of the 1-1/8" API ball is 92.5 grams (0.2039lb). The API ball has a more fluid interface area which increases the sealing pressure when compared to, the alternate ball. Therefore, the smaller the ball, the less work is needed to change the valve's status. A lower amount of work means lower pressure drops in the ball-restricted region.

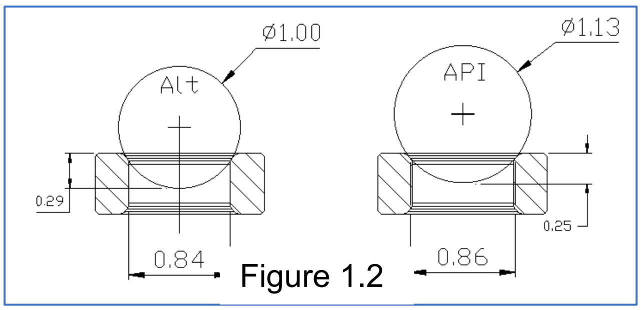

Figure 1.2

The lab test is conducted for (API vs. ALT BALL) described in the lab test method illustrated in **Figure 1.1.** The lab test results compare the API vs. the Alt ball pressure drop with a .155" ball race clearance and a 0.9" ball travel length. The pressure drop values at various flow rates for the API vs. Alt ball is recorded and plotted on the graph. The overall pressure drop curve for the API ball (cage #1) and alternate ball (cage # 2) across nine discrete flow patterns explain the ball restriction experienced with loss in pressure. The higher the pressure drop; the more work is done in the ball restriction region. Work done in this ball restriction area could be used to lift the ball from the seat or rattle the ball while lifting. The outcome of the test setup declares that the alternate ball with the same seat had less pressure drop. This means that the seat with the smaller ball delivers less pressure drop. The alternate ball needs 30% less PIP to open the standing valve.

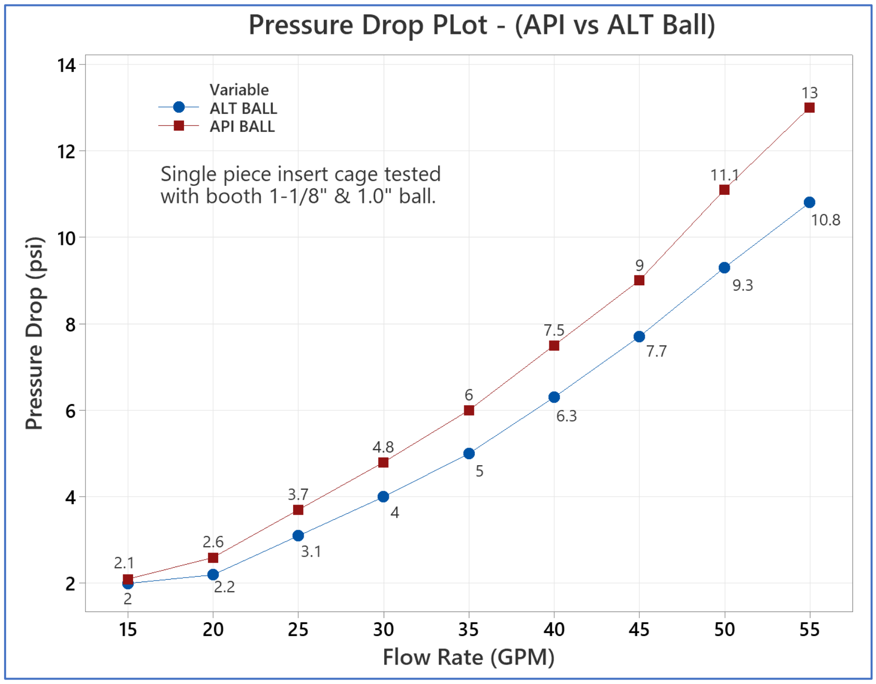

1.2 Pressure drops vs. Ball travel

The work done by the fluid to lift the ball to the fully open position and retain the ball in this open position is the pressure loss experienced by the fluid in the ball-restricted area. The force to lift the ball to the open position (lifting ball self-weight and overcoming sealing pressure) and travel the distance to reach the full open state with respect to the seat sealing surface.

W = Work done to open the cage
w1 = Work done to lift the ball without fluid resistance
w2= Sealing fluid resistance to open
F = Net up lift force applied on the ball
m = Mass of the ball
g = Gravity
s= Ball travel distance
h = Fluid height above the sealing surface
a = Pressure-acting area
PIP = Bottom hole Pressure in psi

$$w1 = m * g * s$$
$$w2 = \rho * g * h$$
$$W = (m * g * s) + (\rho * g * h)$$

The pressure drops across the standing, and traveling valves affect pump fillage, gas breakout, sand separation, pumping rate, and compressive loads on the rod string. Tests conducted as per the lab test method are illustrated in **Figure 1.1.** The graph shows the pressure drop for three different ball travel lengths. In addition, it shows the recorded pressure drop curves at various flow rates for all three types of ball restriction travel lengths (ball race length). The outcome of this test result is that an increase in ball travel (ball race length) increases the pressure drop. The combined effect of the ball diameter and longer traveling distance are leading causes for the increase in pressure drop. The 1.0” ball size with 1.15” travel in the cage configuration has the highest pressure drop, while the short travel of 1.0” ball size with 0.5” travel has the lowest pressure drop.

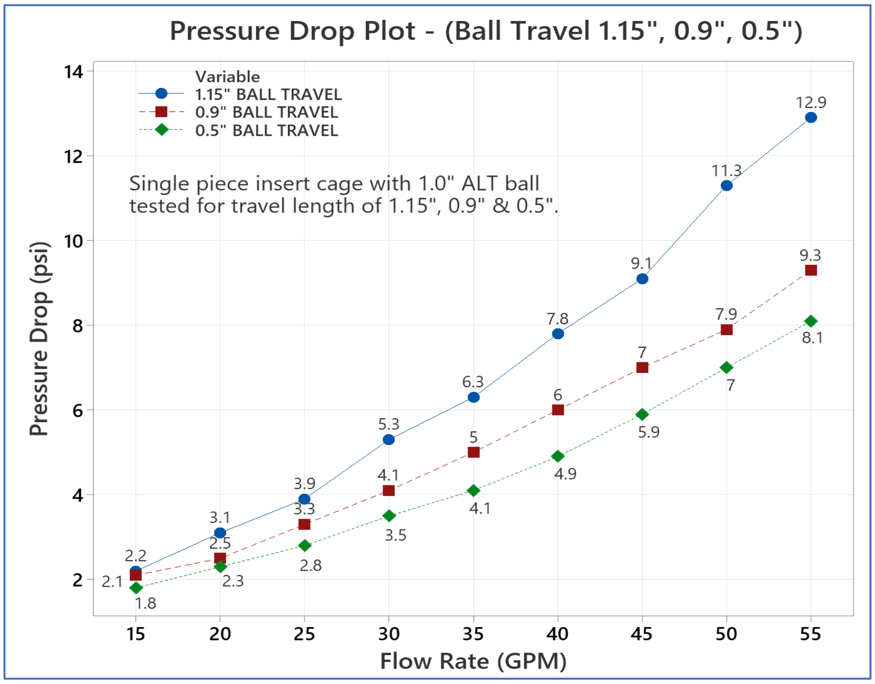

<u>1.3 Pressure drop vs. ball race clearance</u>

The standing and traveling valve in a rod pumped well holds an insert to contain the ball movement inside the valves. The clearance supported between the ball OD and the insert ball race ID defines the ball stability to be coaxial with the cage axis while the cage opens and closes. This clearance also slips off the sand particles carried by the fluid so that it does not get trapped between the clearance. Wells with higher concentrations of coarse sand particles will need smaller clearances for coarse sand not to find the space between the ball OD’s nesting region and the ball race ID. Similarly, the well with higher concentrations of finer sand particles will need more clearance between the ball OD and the ball race ID so that the small sand particles do not get trapped between the nesting region of the ball OD and the ball race ID. The clearance to manage sand particles affects the pressure drop of the cage. The testing described below, and the pressure drop graph plotted from the test setup explains how a larger ball clearance will increase the valve pressure drop.

The graph (Pressure drop due to ball clearance) shows the recorded pressure drops at various flow rates. The graph shows the overall pressure drop curves for all four types of ball race clearances on a cage configuration. The highest-pressure drop is with a ball race clearance of 0.155," and the lowest drop is with a ball race clearance of 0.032". The pressure drop differences for the ball clearances of 0.032" and 0.063" is larger than the pressure drop differences for the ball clearances of 0.062" and 0.155". The mid-range ball race clearance of 0.047" fills the larger gap in-between 0.032" and 0.063". The pressure drop of all four configurations forms a perfect bell curve, which shows that any clearance from 0.016" to 0.11" will have a positive pressure drop slope (increasing). Any clearance above 0.11" will have a negative pressure drop slope (decreasing).

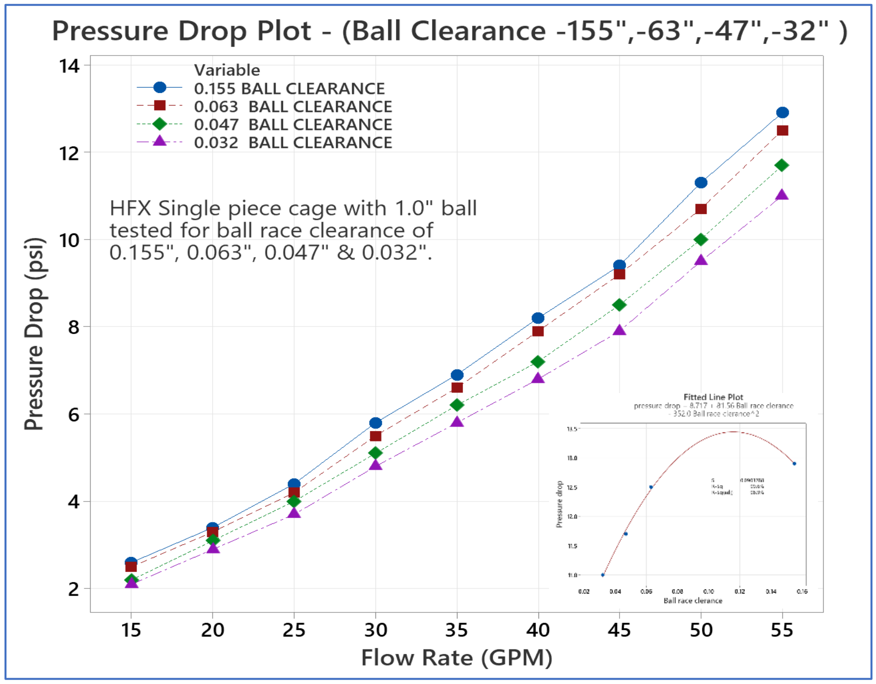

2. Ball net up lifting force & coefficient of lift

The ball lifting force (he Lift = C=½ρV²A – Von-Karman & Wagner Equation) is critical for changes in the cage status from closed to open. The lift force changing the cage status is the product of an inlet cracking pressure acting on the ball area to open the cage. To understand the feature affecting ball lifting force, three concepts were developed to analyze them in finite element analysis. The boundary condition of three conceptual finite element conditions description is next. The ball diameter (1.0"), the ball travel distance (~0.9"), and the ball race clearance remain the same for all three concepts during the single-phase fluid simulation with water properties. However, the actual lab testing to record the cracking pressure had a limitation with the current pressure transducer resolution and the flow measuring sensor missing in the outlet side of the valve (explained in Figure 1.1). Due to these limitations, the netball lift force is validated only with finite element analysis.

The conventional cage is manufactured with a drill out of the cage ID, leaving a 118°F cone feature at the end of the drill, which holds the ball in the open position. The method of a drill cone angle to hold the ball in a rest position is the model shown in concept 1. The fluid flow path is coaxial and parallel to the cage axis. This configuration of concept 1 is used for the finite element analysis in simulating the ball lift force. In concept 2, the ball rest is modified with a spherical cone ball rest that catches the ball in a cone spherical surface area. The webs connecting to support the ball rest are also machined with spherical cone features for additional ball rest support to not rattle the ball during fluid

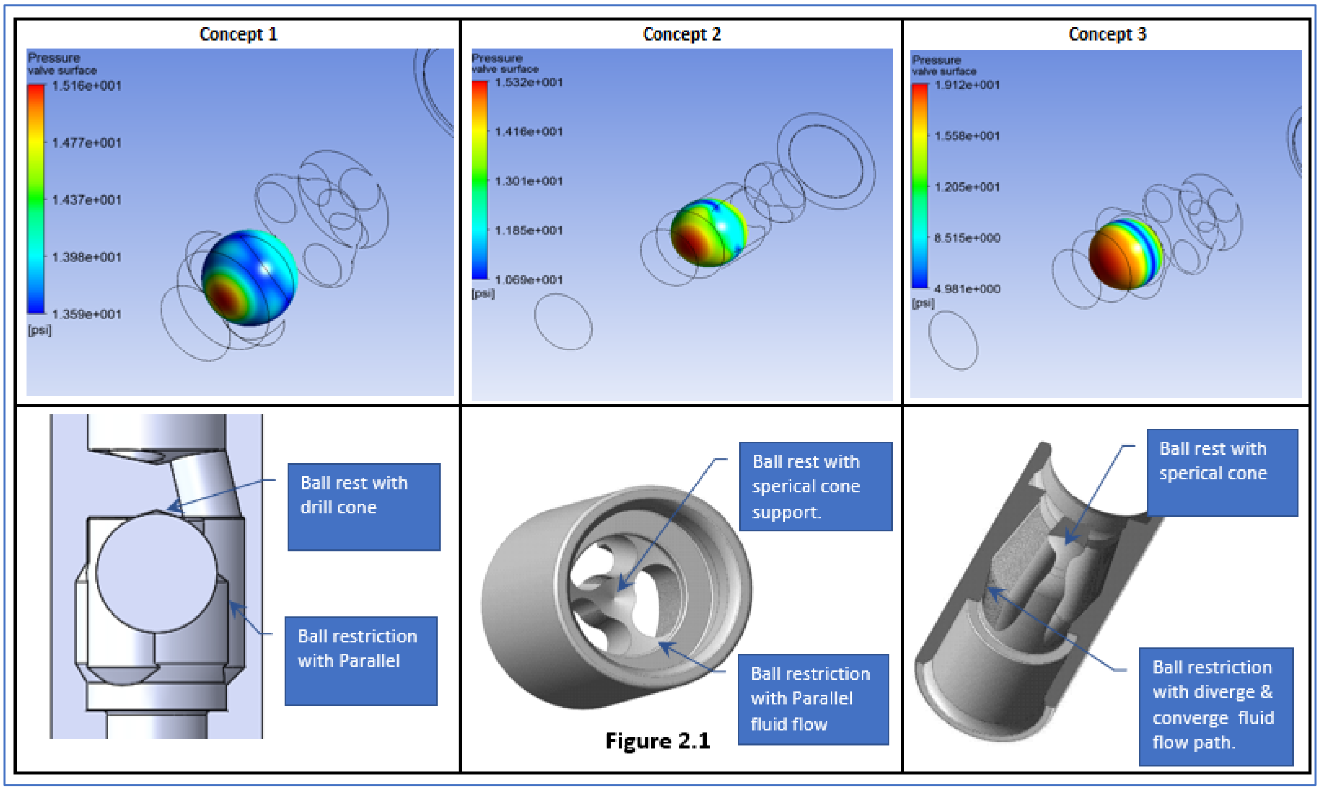

Figure 2.1

flow. The flow path of concept 2 is like concept 1. Concept 3 is like concept 2 regarding the ball rest; however, the fluid flow path is modified with a diverging inlet and converging outlet to maintain the fluid velocity while passing the ball-restricted region. The pictorial simulation and concept features are explained further in **Figure 2.1**.

All three of the concepts explained in **Figure 2.1** were analyzed in the flow simulation condition since the general equation is missing to consider many other parameters related to netball lifting force. For all three concepts, the simulation used a 1.0” ball with a 0.9” ball travel length. Water is the fluid used for this simulation and kept at constant room temperature with a specific gravity of 1.0. The internal valve surface finish was 62Ra, and the ball and seat surface finish were defined as 2Ra for all three concepts to minimize surface fluid friction. The inlet fluid volume is varied through the cage ball resistance, and the inlet pressure to push the volume through the cage resistance is adjusted in psi. Once the test fluid volume is pushed through the cage ball restriction, the ball will experience an uplift force to float the ball in the direction of the fluid flow due to inlet pressure (psi). The uplift force experienced by the ball is recorded for every discrete simulated flow and plotted on the graph for all three concepts. The results of this simulation showed that concepts 1 and 2 have a similar ball lift force with marginal differences, while concept 3 showed a greater ball lift force for all discrete flow rates. This finding confirms the added benefits of the diverge and converge fluid flow path, which maximizes the ball lift force with a higher co-efficient of ball lifting. This ball lift force is critical for the standing valve (SV) application to change from close to open with minimum PIP.

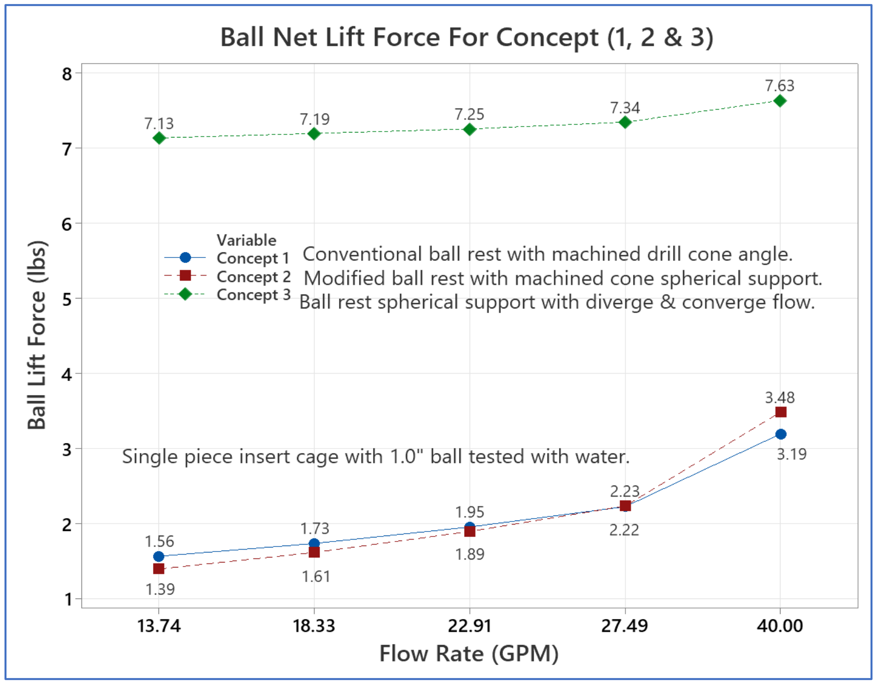

3. Fluid tracing and untracing cage ball surface

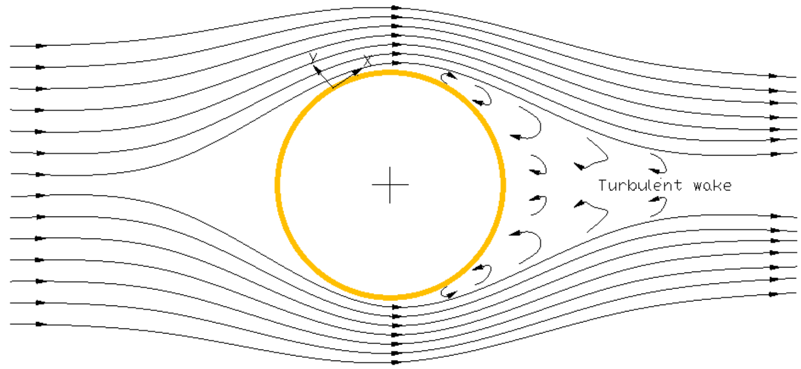

Figure 3.1

Understanding the fluid flow path behavior while tracing the ball surface behavior in a cage is straightforward with a few upfront assumptions. The cage's fluid flow is assumed to have laminar layers with constant fluid density. The fluid friction is negligible and constant over the valve length. The laminar layer of flow lines is linear and does not get separated due to fluid viscosity (molecular adhering force). The fluid flow with velocity (v) can tear the molecular adhering force if the Reynolds number of the fluid is lower, which means that if the fluid velocity is greater than the molecular adhering force, the fluid flowing in that layer can shift or swap to another fluid layer. The Diagram in **Figure 3.1** shows the fluid flow line vector in the "X" axis as the fluid velocity and the vector perpendicular to the fluid flow path in the fluid flow layer depth as the "Y" axis. As the fluid approaches the ball, it will trace the surface until the diameter with a drift in its layer depth vector. After the fluid passes the ball diameter, the fluid layer tracing the ball surface is missing and will create a wake region with turbulent flow. The outermost mechanical boundary layer contributes a lot to controlling the wake region. The wider the space for fluid after passing the ball's diameter, the larger the wake region. If the fluid flow area after the ball's center is narrowed, it will push the fluid layers toward the center and minimize the wake region.

Figure 3.2 shows the fluid tracing ball surface behavior over the fluid path length as the fluid comes close to the ball. The fluid layers deflect and accelerate to catchup to the ball surface trace. When the fluid reaches the fluid path at the center of the ball (max ball diameter), the fluid's acceleration ends, and the fluid's deceleration starts. When the fluid

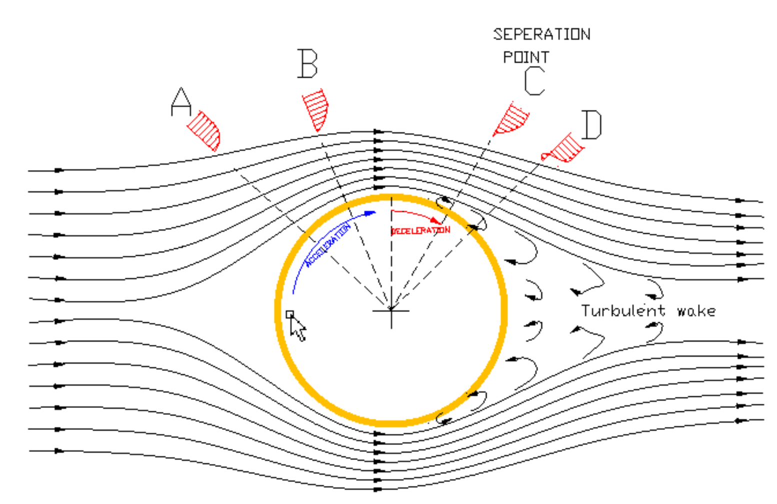

Figure 3.2

decelerates to tracing the ball surface and reaches v=0, the fluid separates from the ball surface tracing and creates a wake region with the turbulent fluid. The fluid paths are optimized with a diverging region while the fluid accelerates to catch up to the ball and with a converging fluid path while the fluid decelerates to separate from the ball's surface. The diverge in the inlet area (near the side of the ball) minimizes the fluid acceleration. The convergence in the outlet (far side of the ball) area narrows the wake region to maximize the lifting force and minimize the pressure drop in the ball's restriction area.

Concept 3, which matches the traveling HFX cage design, is analyzed with a single-phase fluid flow simulation to plot the fluid flow trajectory from the cage inlet to the outlet. Multiple trajectories (approx. 400+) were plotted around the ball's restricted area with multiple layers. Each fluid flow trajectory is color coded to the read velocity value at specific points in the fluid path. The simulation started with an inlet fluid velocity of 10in/sec and with an outlet fluid velocity exit of 11in/sec. The max fluid velocity on the trajectory is in the region aligned with the center of the ball, and the cage is fully open. **Figure 3.4** shows the image of all 400+ fluid flow trajectory points with the colored velocity indication. The fluid flow trajectory at the far side of the ball converges to a single stream flow that leaves a vacant space "wake region." The cage in concept 3 with the spherical ball rests at a fully open position and with an extended cone geometry for the insert fill in the wake region to converge and guide towards the exit. This avoids fluid trajectory rebound back onto the ball due to the fluid untracing the ball surface after reaching escape velocity.

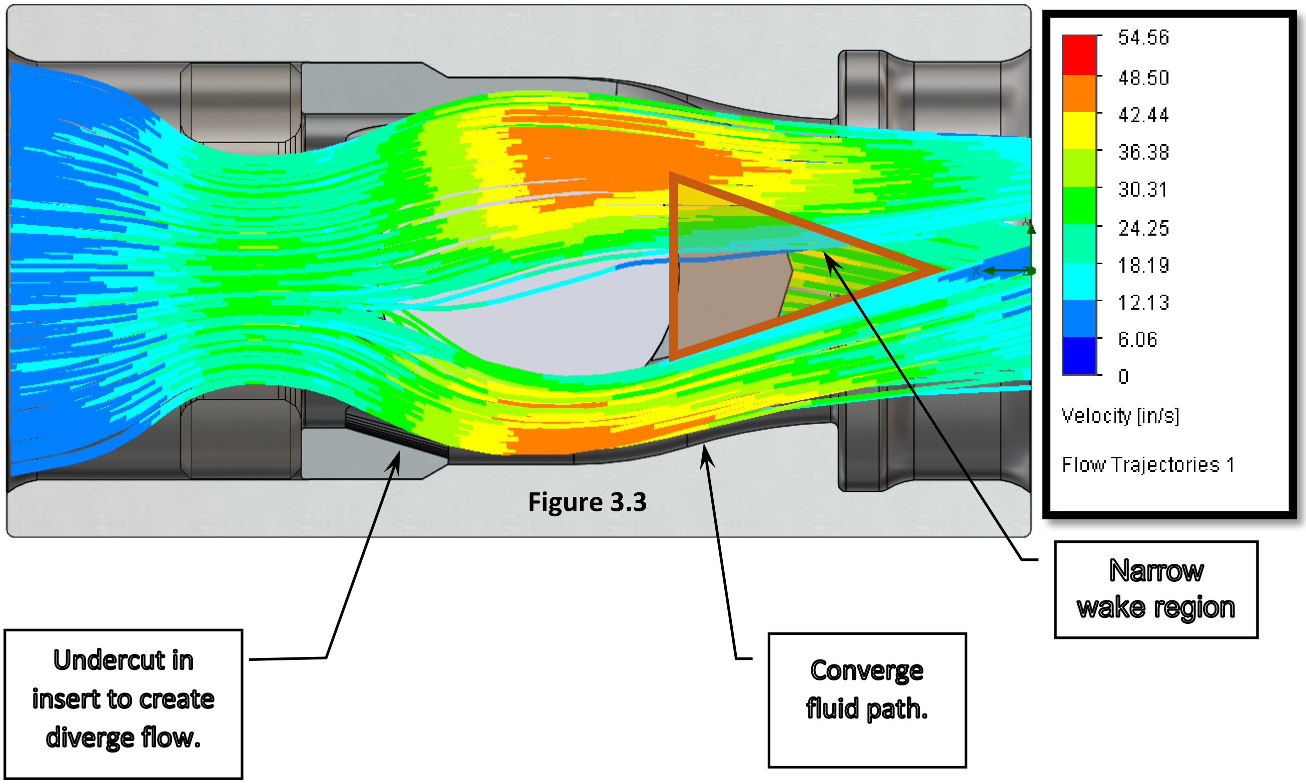

Figure 3.3

4. Change in ball resistance vs. fluid velocity

The flow simulation in section 3 with Figure 3.3 explains that the inlet and outlet fluid velocities are 10 in/sec and 11 in/sec, respectively. The cage reaches a high fluid velocity at the center of the ball when the valve is in a fully open position. The factors impacting a cage's ability to handle multiphase fluid (sand, gas, and oil) are 1) maintain a smooth velocity trajectory for multiphase fluid to pass the ball restriction (resistance) and minimize sudden changes in flow velocity to avoid the separation of multiphase fluid, 2) a fluid layer close to the boundary wall condition will move at a lower velocity while a fluid layer in-between two boundary wall conditions will have max velocity. The velocity plot offset of the fluid layer close to the wall and the fluid layer between the wall to offset with minimum change in the span between them. The greater the span change between the fluid layer close to the wall and fluid layer between layer is a sign that cage cross sectional area is not in conjunction with fluid flow trajectory.

Concepts 2 & 3, explained in section 2, are used to describe the behavior for fluid min & max flow velocity with respect to the fluid flow cross-sectional area in this section. Concept 2 is a parallel spiral flow region with spherical ball seat support at the fully open condition. Concept 3 is the diverge and converge flow region with a spherical ball seat support at the fully open position. **Figure 4.1 & Figure 4.2** are drawn with two Y-Axis scales: the left side Y-axis scale represents fluid velocity (in/sec), and the right-side Y-axis represents the cage fluid flow cross-sectional area (in^2) at the respective location of the cage. The X-axis is the length of the cage with origin from the inlet end, which is typical for both Y-axis scales.

The comparison of Figures 4.2 & 4.3 is to understand better the cage function in terms of the ball restriction and the ability to handle the multiphase fluids and to minimize the change in multiphase fluid properties due to the separation of sand particles and the escape tendencies of dissolved gases. To compare, first identify the ball's center at the fully open position in both figures 4.2 & 4.3, which is shown with a vertical line drawn from the ball center to the graph region to split the graph into two regions of the left and right side. The left side represents the ball restriction entry, and the right represents the ball restriction exit region. The fluid velocity flowing through these regions is important to trespass sand particles and dissolve gasses. The ideal expectation is a slow and gradual increase/decrease in velocity without slipping the sand particles from the flow trajectory. No sudden velocity changes that would create a pressure drop for dissolved gas to escape the fluid.

The graph in Figure 4.1 & 4.2 shows three graphical lines 1) High fluid velocity flowing between wall constraints (orange color). 2) The low fluid velocity of the fluid layer tracing the wall surface (navy blue color). 3) Cross section area of the fluid flow path at each respective point. The fluid velocity span distance between the high and low velocity at the mid-width region of the seat is the left side velocity span. It is named "LS," with a green double arrow vertical line. The span distance between the high and low velocity at the region just after passing the ball's center axis is the reference for the right-side velocity span and is named "RS" with a double arrow vertical light blue color line.

On the left side of the graph with "LS," the velocity difference between the high and the respective low regions are "LVS" compared with "LS". The difference between is LVS-LS =ΔV. this change in velocity span should be minimum for better handling of multiphase fluid. A sudden increase in ΔV at the left side will lower the fluid pressure, and the fluid will experience a sudden pressure change for dissolved gas to escape easily and big sand particles to slip. To minimize the change in ΔV, the left side of the ball should have a smooth area profile ideal for smoothing a spline area graph.

Similar to the left side, "RVS" is compared with "RS." The differences between the two is RVS-RS=ΔV. A sudden or continuous increase in ΔV at the right side will lower the fluid pressure, and the fluid will experience a loss of total pressure for sand particles to be left behind. The ΔV difference at the junction of the left and right sides of the graph is a major contributor of both sand and dissolved gas separation.

Figure 4.1 (Concept 2)

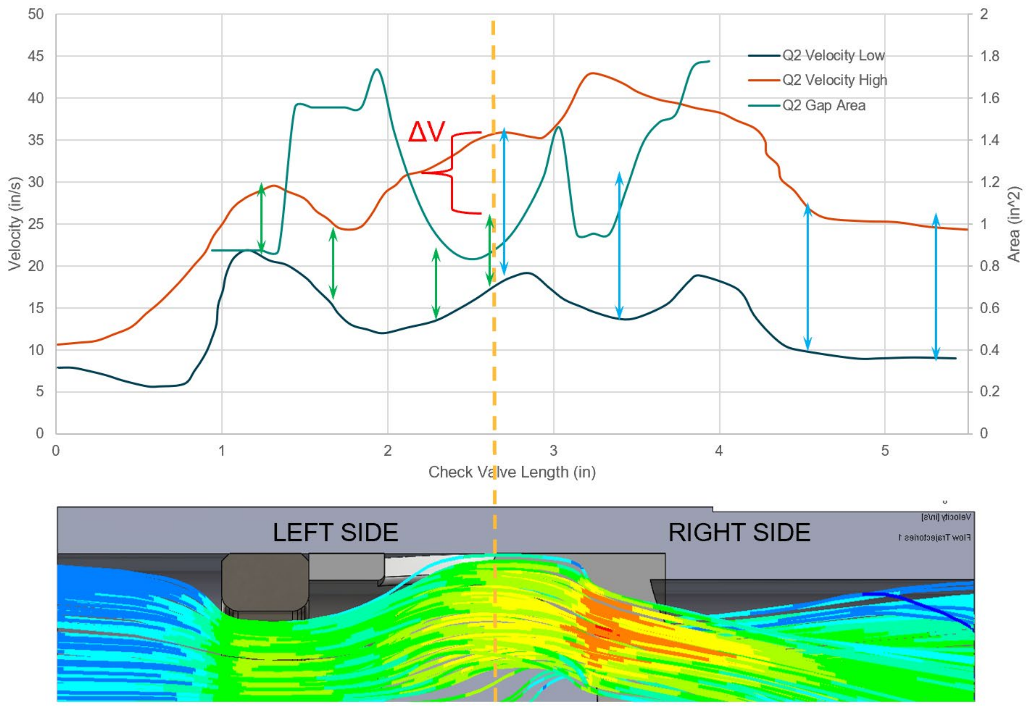

Figure 4.2 (Concept 3, HFX)

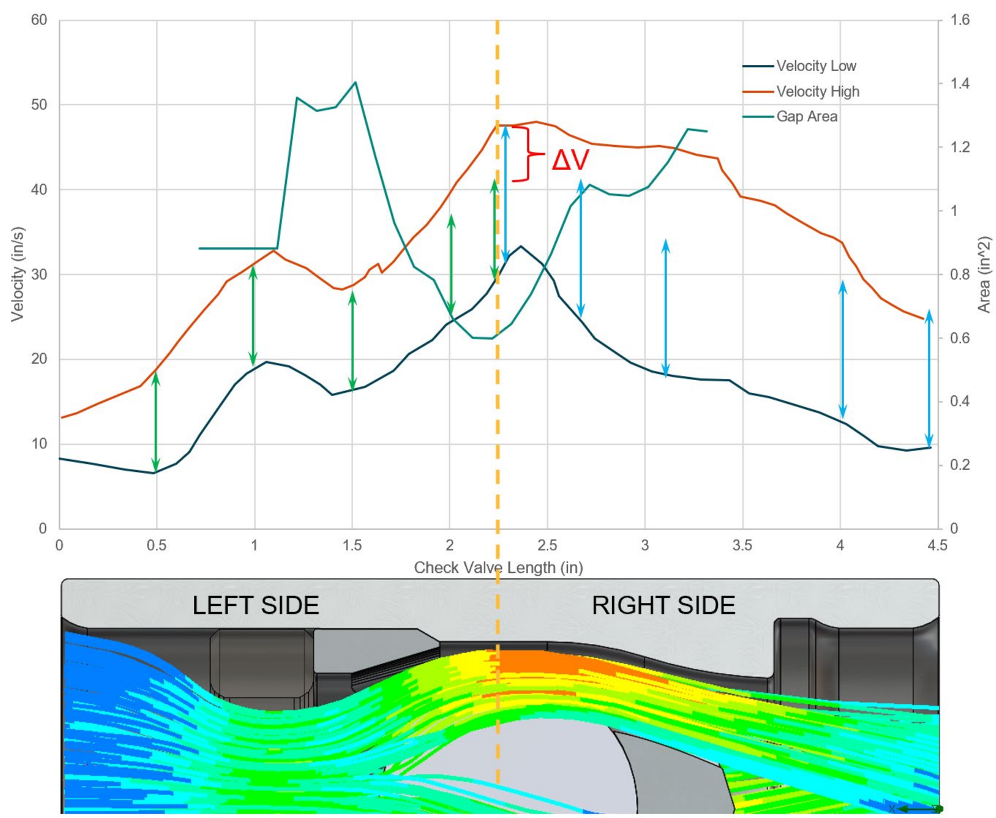

5. Conclusion

Rod pumps are expected to work with gas and solid interference since in today's well operating condition, the system's cages are designed to displace these solids or gas and with minimum overall damage to the rod pump system, ball & seat, ball rattling, fluid pounding, maximizing pump efficiency with fillage, no cage plugging, and a longer run life. Several design features are introduced with the HFX cage to work better with solids and gas to summarize the features explained in all above sections 1) cage with only an alternate ball 2) cage with a ball travel 0.5times of alternate ball ⌀ 3) ball race clearance of -47 in between -32 &-63 4) spherical cone ball rest at full open 5) diverge and converge flow profile 6) very minimal ΔV compared with LS 7) minimum ΔV compared with RS 8)cage material suitable for aggressive environmental operation.

References:

1) Fluid Dynamics Sucker Rod Pump SAND99-0093C
2) "Sarah H Ali et al 2019 J. Phys.: Conf. Ser. 1294 022002" ("Measure liquid viscosity by tracking falling ball Automatically ...")
3) Val-Matic White paper "VM-DSCV/WP"
4) Val-Matic White paper "VM-CAV/WP"
5) IDEX Health & Science white paper "Compressive guide on Check valve"